The College of Engineering
University of Wisconsin-Madison

Wisconsin Electric Machines and Power Electronics Consortium

RESEARCH REPORT
91-17

A Simple and Robust Adaptive Controller for Detuning Correction in Field Oriented Induction Machines

K.T. Hung, T.A. Lipo, R.D. Lorenz
University of Wisconsin-Madison
1415 Johnson Drive
Madison, WI 53706

J.C. Moreira
Whirlpool Company
Monte Road
Benton Harbor, MI 49022

WEMPEC

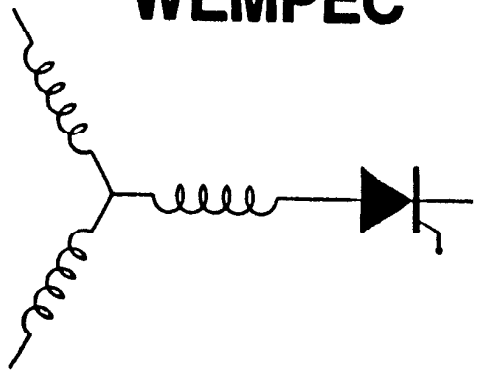

Department of Electrical and Computer Engineering
1415 Johnson Drive
Madison, Wisconsin 53706

A SIMPLE AND ROBUST ADAPTIVE CONTROLLER FOR DETUNING CORRECTION IN FIELD ORIENTED INDUCTION MACHINES

J. C. Moreira
Whirlpool Corporate R&E
Benton Harbor, MI

K. T. Hung
T. A. Lipo
R. D. Lorenz
University of Wisconsin-Madison
Madison, WI

Abstract–This work presents a novel adaptive controller for correcting the rotor time constant estimate used in the slip frequency calculator of indirect field oriented controllers. The controller is novel in that it possess near digital deadbeat performance, and is simultaneously maintains its correctness down to zero speed. The robust controller dynamics are based on an operating point form of digital deadbeat control. In this controller, an operating point approximate inverse model relates changes in the machine parameters to deviation in the rotor flux components. This allows nearly exact, one step (deadbeat) prediction of the correction necessary for the slip calculator gain. The correctness down to zero rotor speed is based on the determination of the rotor flux from an accurate air gap flux estimate obtained from the third harmonic stator phase voltage component introduced by the saturation of the machine stator teeth. Moreover, a function relating the amplitude of the third harmonic air gap flux component with the value of the magnetizing inductance allows correction of this machine parameter for different flux levels. The proposed adaptive controller is implemented in a digital signal processor and the experimental results demonstrate its excellent performance for a wide range of rotor speeds, including locked rotor conditions.

INTRODUCTION

Torque control of alternating current machines, including the induction motor, has drawn considerable attention in the recent years. Both indirect and direct field orientation have been successfully established in theory and practice. In both control strategies the stator current components responsible for the flux and torque production are decoupled via non-linear state feedforward and feedback control loops. This achieves independent and linear control of torque and flux. Since its introduction in the early 80's the direct field orientation scheme has been regarded as less practical because of the sensors needed for obtaining information about the machine variables (e.g. search coils, coil taps, or Hall effect sensors). In addition to increasing the total controller cost, these sensors often impose limitations on the machine operating range. By comparison, indirect field orientation has relatively simpler hardware and better overall performance, especially at low frequencies. A basic implementation of an indirect field orientation controller (IFOC) for an induction motor is shown in Fig. 1 in a simplified block diagram form.

Typically, such controllers utilize machine parameter values (e.g. the rotor time constant and the magnetizing inductance) to implement non-linear feedforward calculation of the proper

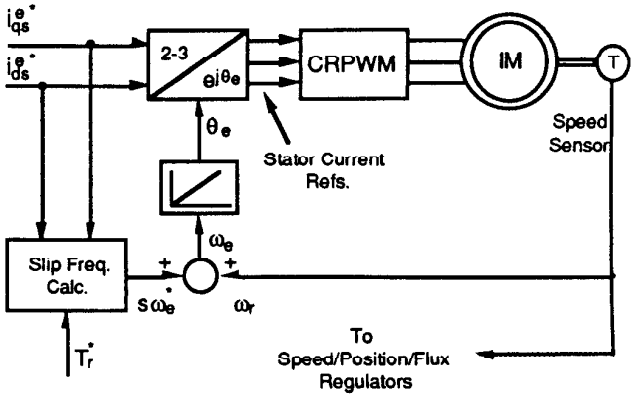

Fig. 1. Implementation of an indirect field orientation controller (IFOC) for induction motor.

motor slip frequency $s\omega_e^*$ so that the conditions for rotor flux orientation, and consequently the decoupling of torque and flux, are achieved. As with all feedforward techniques the decoupling accuracy is parameter dependent. When the rotor time constant, T_r, changes due to temperature or saturation, the decoupling between the control variables is incorrect and the control system operates in a detuned condition. Many methods have been proposed to solve this problem of detuning of the slip calculator, including identification, estimation and adaptation [1-8].

In recent work by Hung and Lorenz [9] and [10] a digital deadbeat adaptive controller was proposed and implemented. In that approach, an operating point, approximate inverse model error function based on the rotor flux error was derived so that the deviation in the slip gain was predicted directly. The resulting adaptive controller can be viewed from a discrete time control point of view in which the feedback correction possesses a dead-beat characteristic allowing short, nearly one-step, convergence times. However, while such a controller removes the sensitivity to rotor parameters, it is sensitive to the stator resistance for low speed operation. This limitation comes from the fact that the non-linear rotor flux observer is based on the stator terminal voltages and currents.

In this paper a new adaptive controller is presented that combines the digital deadbeat adaptive controller presented in [10] with an accurate flux sensing technique based on the saturation third harmonic component of the stator voltages as introduced in [11] and [12]. The resulting controller combines the control robustness and superior performance of

the deadbeat adaptive controller with the accuracy of direct flux sensing. This combination is shown to be practically independent of machine parameters and to exhibit superior performance compared to previous detuning correction solutions. The experimental results demonstrate the robustness of the controller over a wide range of rotor speed, including zero speed for which the slip calculator gain can still be be tuned to its correct value.

The following sections describe the methodology of estimating the rotor flux from the stator third harmonic voltage, the methodology for deadbeat disturbance rejection control design, the derivation of an approximate inverse deadbeat control model for the induction motor, the implementation of the deadbeat adaptive controller, and the experimental results on an induction motor field oriented drive system.

ESTIMATION OF ROTOR FLUX VIA THE SATURATION THIRD HARMONIC

As described in detail in [11] and [12], induction machines are designed to work in the saturation region of the B-H characteristic of their magnetic core material. As a consequence of saturation, the teeth with the highest flux density will saturate and the air gap flux distribution will assume a flattened sinusoidal form with peak value B_{sat} as shown in Fig. 2.

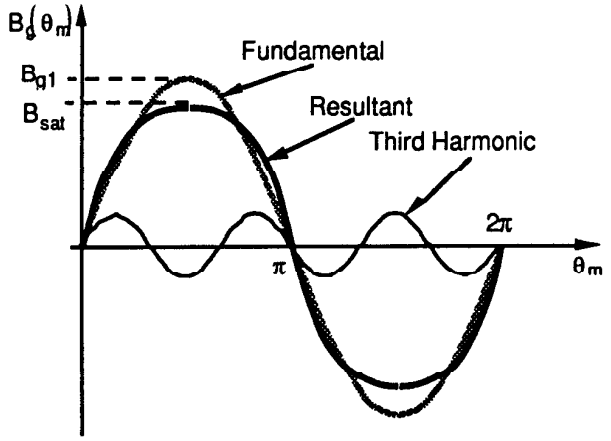

Fig. 2 Actual air gap flux density distribution for an induction machine operating at rated voltage (heavy line). Its fundamental and third harmonic components are also shown.

The flattening of the sine wave of the air gap flux density is produced by the non-linear magnetic B-H curve of the steel. This flattening causes a third harmonic flux component. Consequently, the third harmonic of the air gap flux links the stator winding and induces a third harmonic component in each one of the stator phase voltages that are all in phase, forming a zero sequence set of voltages. If the stator phases are star connected, no third harmonic currents will circulate in the stator side and no third harmonic voltage drop will exist in the stator impedance. Therefore, the stator third harmonic voltage will always be in phase with the third harmonic voltage component of the air gap voltage regarding the load condition of the induction machine. This fact is especially important when locating the position of the fundamental component of the air gap flux with respect to the stator current, as will be discussed later.

When the three stator phase voltages are summed, the fundamental and characteristic harmonics are cancelled and the resultant waveform contains mainly a third harmonic component and a high frequency component due to the rotor slots. This resultant third harmonic voltage term, v_s3, can be integrated so that the resulting flux signal , λ_3 , has an amplitude that can be related to the fundamental amplitude of the air gap flux, λ_{am} or λ_m ,via a saturation function, f_λ , as in Eq. (1).

$$|\lambda_{am}| = f_\lambda(|\lambda_3|) \tag{1}$$

This saturation function is easily obtained experimentally from the results of a conventional no-load test.

The relative position of the fundamental component of the air gap flux with respect to the stator current is obtained by measuring the phase displacement between two fixed points in the third harmonic flux and the line current. Figure 3 shows this phase displacement, γ_{im}, between the maximum values for the fundamental components of current and air gap flux.

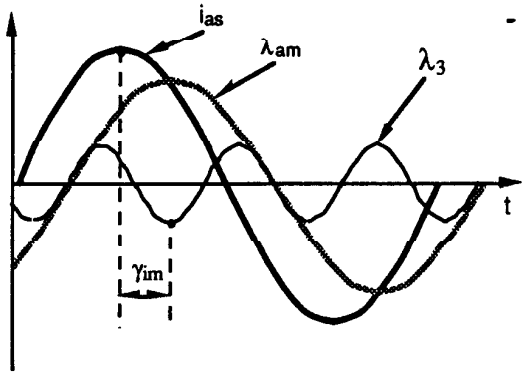

Fig. 3 Fundamental components of stator line current, i_{qs}, fundamental air gap Flux (λ_{am}) and third harmonic flux (λ_3) components. γ_{im} is the phase displacement between the stator current and air gap flux

The fundamental and third harmonic components of the air gap flux, and the stator current are depicted in Fig. 4 in a synchronously rotating reference frame representation, for a condition of field orientation.

It is clear from this vector arrangement that the air gap flux, after having its amplitude $|\lambda_m|$ and its relative position γ_{im} estimated from the third harmonic flux and current signals, can be resolved into its d and q components according to,

$$\lambda_{dm}^{e} = -|\lambda_m^{e}|\sin(\theta_{is}+\gamma_{im}) = -f_\lambda(|\lambda_3^{e}|)\sin(\theta_{is}+\gamma_{im}) \tag{2}$$

$$\lambda_{qm}^{e} = |\lambda_m^{e}|\cos(\theta_{is}+\gamma_{im}) = f_\lambda(|\lambda_3^{e}|)\cos(\theta_{is}+\gamma_{im}) \tag{3}$$

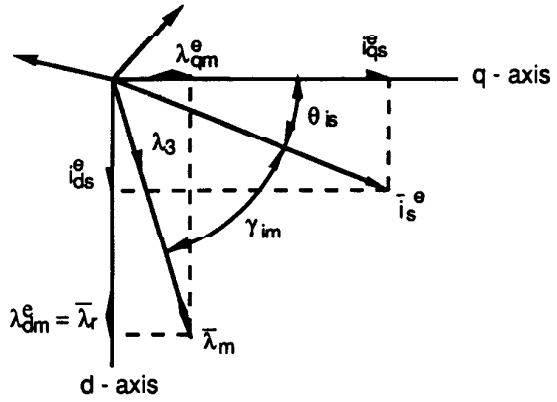

Fig. 4 Stator current, air gap flux, and third harmonic voltage vectors in the synchronous reference frame for a rotor flux orientation condition .

with θ_{is} computed from the reference values for the stator currents, $i_{qs}{}^{e*}$ and $i_{ds}{}^{e*}$ as indicated by (4),

$$\theta_{is} = -\tan^{-1}\left(\frac{i_{ds}{}^{e*}}{i_{qs}{}^{e*}}\right) \tag{4}$$

The rotor flux components can be derived as a function of the air gap flux and stator current components as in the following equations,

$$\lambda^e_{qr} = \frac{\hat{L}_r}{\hat{L}_m}\lambda^e_{qm} - \hat{L}_{lr}\, i^e_{qs} \tag{5}$$

$$\lambda^e_{dr} = \frac{\hat{L}_r}{\hat{L}_m}\lambda^e_{dm} - \hat{L}_{lr}\, i^e_{ds} \tag{6}$$

where $\hat{L}_r$, $\hat{L}_m$, and $\hat{L}_{lr}$, represent, respectively, the estimates for the rotor, magnetizing, and rotor leakage inductances. Although dependent on machine parameters, the rotor flux can be obtained with reasonable accuracy since the rotor leakage inductance $\hat{L}_r$, and the ratio $\hat{L}_r / \hat{L}_m$ are only moderately dependent on the saturation level. Changes in the magnetizing inductance with flux or load levels can be corrected via a function relating the actual value of the magnetizing inductance with the magnitude of the third harmonic flux component, readily obtained from the the function relating the air gap flux and third harmonic flux amplitudes described by (1). This, together with the fact that the rotor leakage inductance can be assumed to be practically constant for normal operating conditions, guarantees a very good robustness for the estimation of the rotor flux for a wide speed range.

DEADBEAT DISTURBANCE REJECTION CONTROL DESIGN

The basic principles of deadbeat control are usually understood as a closed loop discrete time system is achieves a one sample period delay between command and response. This is equivalent to a closed loop transfer function of

$$\frac{\emptyset}{\emptyset^*} = z^{-1} \tag{7}$$

or a difference equation model

$$\emptyset(k) = \emptyset^*(k\text{-}1) \tag{8}$$

Such a controller can be designed for a general closed loop system with a disturbance input as that shown in Fig. 5

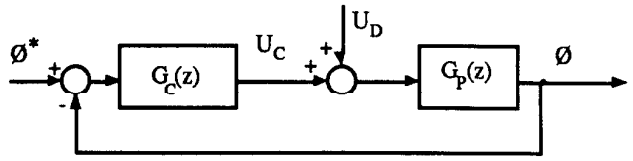

Fig. 5 A z-transform, discrete time, closed loop control system with command $\emptyset^*$ and a disturbance input U_D.

For this closed loop system, the command response is

$$\frac{\emptyset}{\emptyset^*} = \frac{G_c(z)\, G_p(z)}{1 + G_c(z)\, G_p(z)} \tag{9}$$

Combining (7) and (8) yields the required deadbeat controller

$$G_c(z) = G_p(z)^{-1}\, \frac{z^{-1}}{1 - z^{-1}} \tag{10}$$

This deadbeat command response controller consists of two parts:

$G_p(z)^{-1}$ an inverse model of the process and

$\frac{z^{-1}}{1 - z^{-1}}$ a one step delayed integration process.

It is important to note that the deadbeat controller uses

- the inverse model of the process to calculate the input, U_C, required to produce the desired output, $\emptyset^*$.
- the integration process to hold that value of U_C to maintain the desired output, $\emptyset^*$.

This same block diagram can be reformulated as shown in Fig. 6 to show a disturbance input, U_D, and the closed loop controller's disturbance correction response, U_C.

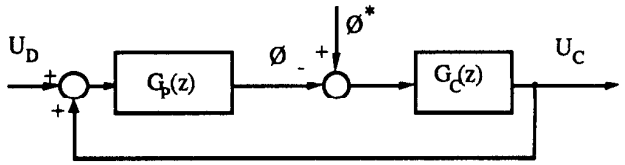

Fig. 6 A z-transform, discrete time, closed loop control system with disturbance input U_D and a command $\emptyset^*$.

This form shows how the closed loop control system can be thought of as a means of producing a correction response to a disturbance input. The best possible correction response is deadbeat, just as it was for the command-driven form. In this case that would imply a difference equation model

$$U_C(K) = U_D(K\text{-}1) \tag{11}$$

This closed loop transfer function is the same as (8), i.e.

$$\frac{U_c}{U_D} = \frac{G_c(z)\, G_p(z)}{1 + G_c(z)\, G_p(z)} \tag{12}$$

Thus, for deadbeat disturbance correction response the controller is exactly the same as (10).

If this controller, Eq. (10), is applied, the output response to a disturbance would be

$$\emptyset(z)\Big|_{\text{dist. resp.}} = U_D(z) \cdot G_p(z) \cdot (1 - z^{-1}) \qquad (13)$$

If the open loop disturbance response, $U_D(z) \cdot G_p(z)$ varies slowly, then after one sample period, the net effect is nearly cancelled by the subtraction action

$$\emptyset(K)\Big|_{\text{dist. resp.}} = U_D G_p(K) - U_D G_p(K-1) \qquad (14)$$

Thus, this form of deadbeat controller can virtually eliminate the error response after one time sample.

This simplified model can now be replaced by a slip gain form of the field oriented controller as shown in Fig. 7.

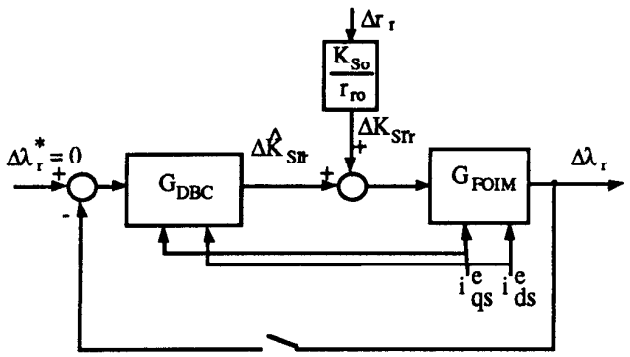

Fig. 7 A slip gain error driven, discrete time, closed loop control system with disturbance input Δr_r, FOIC denotes Field Oriented Induction Motor, DBC = Dead Beat Controller.

This model shows how the unknown change in rotor resistance, Δr_r produces a slip gain disturbance, ΔK_{Srr}. This slip gain disturbance also produces a change in rotor flux, $\Delta\lambda_r$, from the commanded values of

$$\lambda_{dr} = \lambda_{dr}^*, \quad \lambda_{qr}^* = 0 \qquad (15)$$

Since this model is analogous to the general model used for deadbeat design analysis, it should be apparent that for deadbeat disturbance rejection, i.e.

$$\frac{\Delta\hat{K}_{Srr}}{\Delta K_{Srr}} = z^{-1} \qquad (16)$$

the corresponding controller would be

$$G_C(z) = G_{FOIM}(z)^{-1} \frac{z^{-1}}{1 - z^{-1}} \qquad (17)$$

This result confirms that deadbeat disturbance rejection response properties for slip gain errors can be obtained if an inverse model of the field oriented induction machine can be formed and used in the controller. Because the machine model is non-linear, the inverse model will be a linearized, operating point model. Thus the controller will produce "near deadbeat" response. The derivation of this inverse model is the subject of the following section.

APPROXIMATE INVERSE, DEADBEAT CONTROLLER MODEL FOR THE FIELD ORIENTED INDUCTION MACHINE

The basic principle of this controller, as discussed in [9] and [10], is to measure the rotor flux error for use as a feedback signal to the deadbeat controller which computes the slip frequency correction needed, $\Delta\hat{K}_{Srr}$. The rotor flux error relationship to the slip gain error when detuning occurs is the key point in the implementation of the deadbeat adaptive controller. The two rotor flux components are affected by any amount of detuning due to changes in the machine parameters as the following analysis demonstrates.

The q-axis rotor voltage for a squirrel cage induction motor can be written as,

$$0 = r_r i_{qr}^e + p\lambda_{qr}^e + \omega_s \lambda_{dr}^e \qquad (18)$$

Because the detuning is mainly caused by changes in the rotor resistance which occur at a slow rate it is a reasonable approximation to assume that the term $p\lambda_{qr}^e$ is close to zero. Hence, (18) above can be rewritten as,

$$0 = r_r i_{qr}^e + \omega_s \lambda_{dr}^e \qquad (19)$$

The q-axis rotor flux for a non-saturated machine is given by,

$$\lambda_{qr}^e = L_m i_{qs}^e + L_r i_{qr}^e \qquad (20)$$

and solution for the slip frequency ω_s from (19) after substituting i_{qr}^e from (20), yields

$$\omega_s = \frac{L_m}{T_r} i_{qs}^e \lambda_{dr}^{e\,-1} - \frac{1}{T_r} \lambda_{qr}^e \lambda_{dr}^{e\,-1} = m i_{qs}^e \lambda_{dr}^{e\,-1} - n \lambda_{qr}^e \lambda_{dr}^{e\,-1} \qquad (21)$$

With the machine operating under field orientation the commanded slip frequency $\omega_s^* = \omega_s$, and the estimates $\hat{m}$ and $\hat{n}$ coincide with the actual values for m and n in the equation above, as shown by

$$\omega_s^* = \hat{m} i_{qs}^* \lambda_{dr}^{e\,*-1} \qquad (22)$$

where the q-axis component of the rotor flux is zero.

When a detuning condition occurs an error in the parameter estimates appears as well as in the rotor flux components, such that the slip frequency given by (21) becomes,

$$\omega_s = (\hat{m} + \Delta m)\left(\lambda_{dr}^{e\,*-1} - \Delta\lambda_{dr}^{e\,-1}\right) i_{qs}^e - \ldots$$
$$(\hat{n} + \Delta n)\left(\lambda_{qr}^{e\,*} + \Delta\lambda_{qr}^e\right)\left(\lambda_{dr}^{e\,*-1} - \Delta\lambda_{dr}^{e\,-1}\right) \qquad (23)$$

which after identifying the terms that correspond to the definition for ω_s reduces to,

$$0 = \Delta m \lambda_{dr}^{e\,*-1} i_{qs}^e - \hat{m}\Delta\lambda_{dr}^{e\,-1} i_{qs}^e - \hat{n}\lambda_{dr}^{e\,*-1}\Delta\lambda_{qr}^e \qquad (24)$$

Alternatively, the expression for Δm above can be expressed in terms of the actual d-axis rotor flux instead its reference value as,

$$\frac{\Delta m}{\hat{m}} = \frac{\Delta\lambda_{dr}^e}{\lambda_{dr}^e} + \frac{\Delta\lambda_{qr}^e}{\hat{L}_m i_{qs}^*} \qquad (25)$$

As a result, the deviation in the parameter estimation represented by Δm is readily computed as a function of the error in the d and q components of the rotor flux. This error is used by the controller algorithm to compute the necessary change in the slip gain commanded to the slip frequency

calculator. When Δm is added to the estimate $\hat{m}$, (22) yields,

$$\omega_s^* = (\hat{m} + \Delta m)\, i_{qs}^{e\,*} \lambda_{dr}^{e\,*\,-1} = (K_s^* + \Delta K_s)\, i_{qs}^{e\,*} \tag{26}$$

where the symbol K_s^* is the rated slip gain computed from (27), and ΔK_s is its variation obtained from (25).

$$K_s^* = \hat{m}\, \lambda_{dr}^{e\,*\,-1} = \frac{\hat{L}_m}{T_r^*} \frac{1}{\lambda_{dr}^{e\,*}} \tag{27}$$

IMPLEMENTATION OF A NEARLY DEADBEAT ADAPTIVE CONTROLLER

Figure 8 illustrates the experimental indirect field oriented control (IFOC) drive system which has been implemented. Both the adaptive and the field orientation control algorithms are implemented using a digital signal processor with two look-up tables containing the non-linear functions $f\lambda$ and fLm. The sample rate for the deadbeat control loop was 10 Hz, deemed sufficient for rotor resistance thermal dynamics.

EXPERIMENTAL RESULTS

Figure 9 shows the third harmonic stator voltage signal obtained from the summation of the three phase voltages for operation at no load and synchronous frequency around 30 Hz. A current regulated PWM inverter is used to supply the induction machine. Figure 9-a shows the third harmonic voltage and one of the line currents. The switching frequency component in the third harmonic voltage can be easily eliminated by a low pass filter (LPF). Another LPF is used

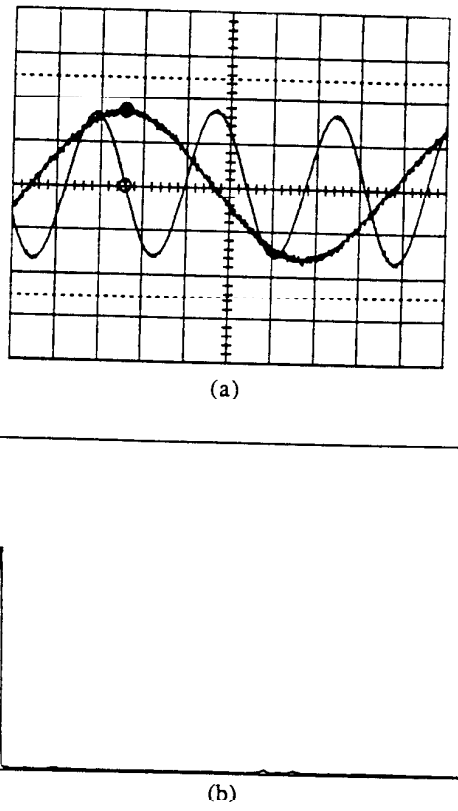

Fig. 9 Experimental results obtained for the test motor. (a) line current (1 Amp/Div.) and stator third harmonic voltage (5 Volt/Div.), Hor: 4ms/div. (b) third harmonic voltage spectrum (full scale of 10 Volts-rms), freq: 0-2000Hz full scale.

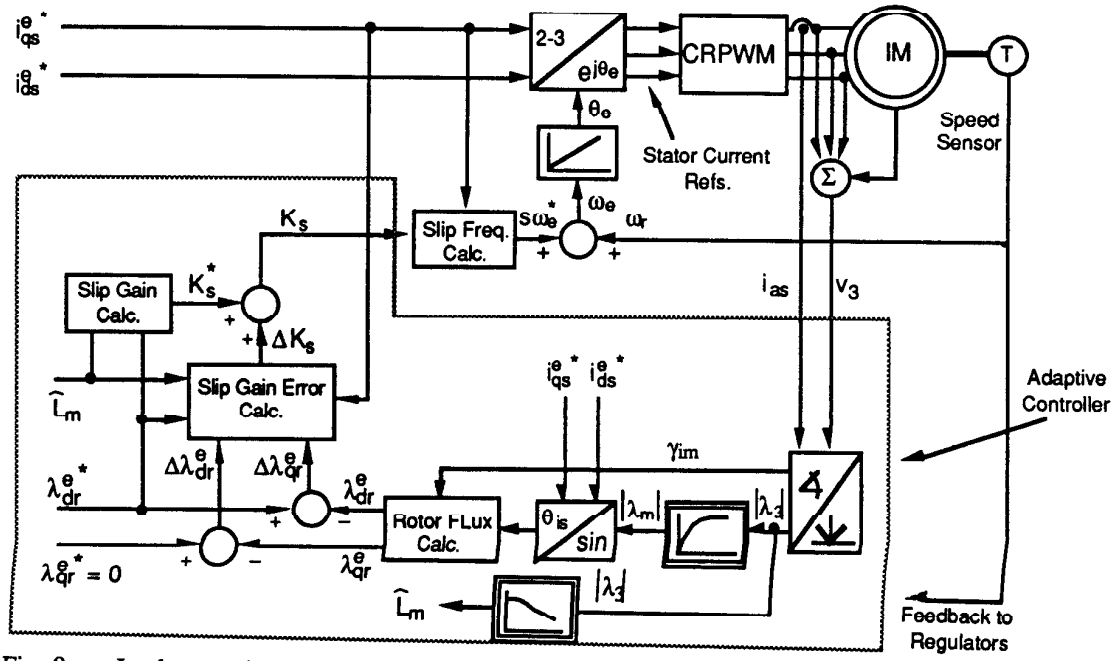

Fig. 8 Implementation of the nearly deadbeat, adaptive IFOC controller for the rotor time constant with the magnetizing inductance estimate based on the amplitude of the third harmonic voltage signal.

for the current so that the phase displacement between the current and third harmonic voltage is kept at its original value. It can be verified that the two points shown in the figure correspond to the maximum values for the air gap flux and current, since the zero crossing for the voltage waveform corresponds to a maximum value for the flux.

As expected for a no-load condition, the phase shift between these two points, which represents the phase shift between the fundamental components of air gap flux and stator mmf, is very small since the mechanical output power developed is only to overcome the windage and friction losses. As the machine is loaded this phase shift increases to respond to the torque required by the load. As mentioned before, the high frequency components in the third harmonic are easily eliminated by a simple filter, making this signal convenient for analog or digital processing.

The spectrum contents for the third harmonic signal is analyzed and shown in Fig. 9-b. As predicted, after the summation of the three phase voltages all the polyphase components are eliminated and the third harmonic is clearly the dominant component at the lower side of the frequency spectrum. The PWM inverter utilized for these measurements has a variable switching frequency (3- 5 kHz) which may have an amplitude comparable with the third harmonic signal and needs, hence, to be filtered. The nearly deadbeat controller of Fig. 8 was implemented in the laboratory and Figs. 10, 11 and 12 show some of the experimental results.

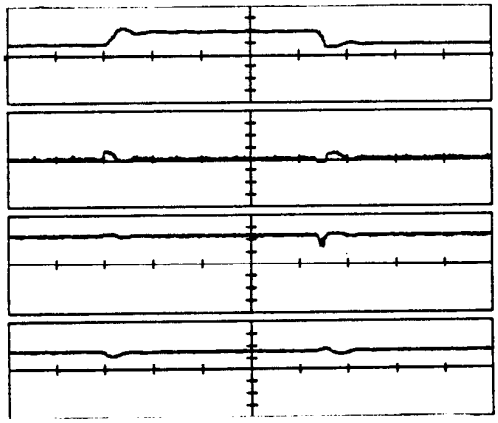

Fig. 10 Experimental results for the nearly deadbeat adaptive controller implemented in an IFOC driving the test motor at rated torque and rated flux commands. The rotor resistance is doubled at 4 seconds (step change) and returned to its nominal value after about 9 seconds (step change).
From top to bottom: (Hor: 2 s/div)
(i) slip gain (10 Hz/A/div),
(ii) q-axis component of the rotor flux (0.2 V.s/div),
(iii) d-axis component of the rotor flux (0.2 V.s/div), and
(iv) mechanical speed (300 rpm/div).

Figure 10 shows (from top to bottom) the evolution of the slip gain, the q-axis component of the rotor flux, the d-axis component of the rotor flux, and mechanical speed. Theis data was taken for a test motor coupled to a dynamometer running at rated torque andflux. The rotor resistance was doubled initially and then returned to the nominal value (both step changes). The correction for the slip gain is very fast, taking less than 2 seconds for the controller to command the right slip gain. Note that the response of the system for the two changes of the rotor resistance is slightly different. This is a consequence of the non linearity which is not exactly modelled in the "nearly" deadbeat controller.

To investigate the third harmonic sensing capability at low flux levels, the same test described in Fig. 10 was carried out with a flux command of 50% of the rated value with the results shown in Fig. 11. These results demonstrate that even at reduced levels of saturation the third harmonic signal remains useful for estimating the rotor flux .

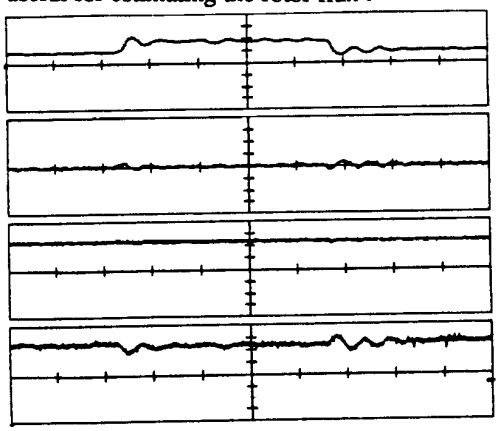

Fig. 11 Experimental results for the nearly deadbeat adaptive controller implemented in an IFOC driving the test motor at rated torque and 50% flux commands. The rotor resistance is doubled at 4 seconds (step change) and returned to its nominal value after about 9 seconds (step change).
From top to bottom: (Hor: 2 s/div)
(i) slip gain (10 Hz/A/div),
(ii) q-axis component of the rotor flux (0.2 V.s/div),
(iii) d-axis component of the rotor flux (0.2 V.s/div), and
(iv) mechanical speed (300 rpm/div).

Fig. 12 shows the nearly ideal performance of the experimental controller under locked rotor conditions at rated torque and rated flux values.The results show that even at zero speed (*locked rotor*) the nearly deadbeat controller achieves excellent dynamic performance and that the third harmonic flux estimation makes the tuning correct independent of the stator impedance at low speeds. The same variables shown in the previous figure are shown again in this figure for the same amount of change in the rotor resistance as for the case above. The system has an excellent response, not matched by previous reported controllers operating at these same conditions. Note that the error generated in the rotor flux components and the type of response are essentially the same as for the case in Figs. 10 and 11.

ACKNOWLEDGMENTS

This work was supported in part by the Wisconsin Electric Machines and Power Electronics Consortium, WEMPEC, in the Department of Electrical And Computer Engineering at the University of Wisconsin-Madison, Madison, Wisconsin.

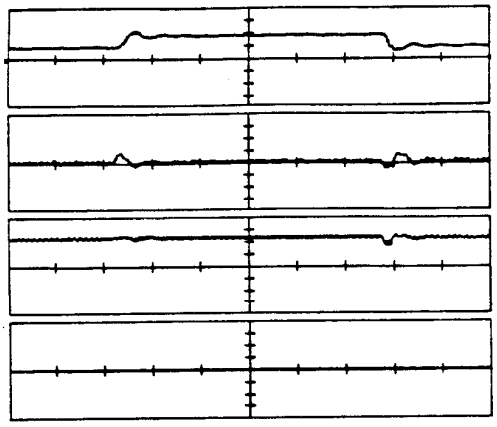

Fig. 12 Experimental results for the nearly deadbeat controller implemented as part of an indirect field orientation controller driving the test motor at rated torque and rated flux commands at zero speed. The rotor resistance is doubled at a time approximately 4 seconds (step change) from the beginning of the trace and returned to its nominal value after about 12 seconds (step change).

From top to bottom: (Hor: 2 s/div)

(i) slip gain (10 Hz/A/div),

(ii) q-axis component of the rotor flux (0.2 V.s/div),

(iii) d-axis component of the rotor flux (0.2 V.s/div), and

(iv) mechanical speed (zero rpm)

CONCLUSIONS

A simple and robust method for correcting the rotor time constant in indirect field oriented control of induction machines has been presented. The adaptive controller proposed is based on a nearly deadbeat structure which has the objective of eliminating rotor flux disturbances by commanding the correct slip gain as predicted from an approximate inverse model of the machine.

In addition to excellent dynamics, the nearly deadbeat controller is made accurate by the measurement of the air gap flux from the third harmonic component of stator voltage and estimation of the rotor flux.

This method also requires knowledge of the machine magnetizing inductance which can not be considered a constant under practical circumstances. Therefore, a correction strategy for changes in the magnetizing inductance with flux level is implemented in the controller. This correction strategy is based on a function relating the value of the inductance with the amplitude of the third harmonic flux signal. Consequently, the controller becomes independent of variations of the magnetizing inductance.

The experimental implementation of the nearly deadbeat controller has used a Motorola 56001 digital signal processor. However the DSP speed was not needed for this loop since a 10 Hz sample rate was used for the deadbeat controller. This controller was part of part of a DSP-based indirect field oriented drive used with a wound rotor induction motor. The system clearly has excellent response for speeds ranging from *zero* to twice the rated value, unmatched by previous reported controllers operating under the same conditions.

TABLE I: TEST INDUCTION MOTOR PARAMETERS

Quantity	Symbol	Value
Line Voltage	Vl	220 V rms
Output Power	P_o	1/3 HP
Speed	ω_r	1725 rpm
Poles	P	4
Frame	-	56T60
Stator resistance	r_s	7.15Ω
Rotor resistance	r_r	6.0Ω
Stator leakage reactance	X_{ls}	5.14 Ω
Rotor leakage reactance	X_{lr}	3.23 Ω
Unsaturated mag. reactance	X_m	100.65 Ω
Rotor Inertia	J_m	0.022 Kg-m^2
Number of rotor slots	n_r	33
Number of stator slots	n_s	36
Air gap length	g_o	1.28 mm
Rotor skew	–	1 slot
Stator pole pitch	τ_s	7/9
Rotor Stack length	l_m	46.18 mm

REFERENCES

[1] L.J. Garces, "Parameter Adaption for the Speed-Controlled Static AC Drive with a Squirrel-Cage Induction Motor", *IEEE Trans. on Industry Applications*, Vol. 16, No.2, March/April 1980, pp. 173-178.

[2] T. Matsuo and T.A. Lipo, "A Rotor Parameter Identification Scheme for Vector-Controlled Induction Motor Drives", *IEEE Trans. on Industry Applications*, Vol. 21, No.4, May/June 1985, pp. 624-632.

[3] K.B. Nordin, D.W. Novotny, and D.S. Zinger, "The Influence of Motor Parameter Deviations in Feedforward Field Orientation Drive Systems", *IEEE Trans. on Industry Applications*, Vol. 21, No.4, July/August 1985, pp. 1009-1015.

[4] L.C. Zai and T.A. Lipo, "An Extended Kalman Filter Approach to Rotor Time Constant Measurement in PWM Induction Motor Drives", *1987 IEEE Industry Applications Soc. Annual Meeting*, October 1987.

[5] H. Sugimoto and S. Tamai, "Secondary Resistance Identification of an Induction-Motor Applied Model Reference Adaptive System and Its Characteristics", *IEEE Trans. on Industry Applications*, Vol. 23, No.2, March/April 1987, pp. 296-303.

[6] C. Wang, D.W. Novotny, and T.A. Lipo, "An Automated Rotor Time Constant Measurement System for Indirect Field-Oriented Drives", *IEEE Trans. on Industry Applications*, Vol. 24, No.1, January/February 1988, pp. 151-159.

[7] R.D. Lorenz and D.B. Lawson, "A Simplified Approach to Continuous On-Line Tuning of Field Oriented Induction Machine Drives", *1988 IEEE Industry Applications Soc. Annual Meeting*, 1988 pp. 444-449.

[8] T.M. Rowan, R.J. Kerkman and D. Leggate "A Simple On-Line Adaption for Indirect Field Orientation of an Induction Machine", *1989 IEEE Industry Applications Soc. Annual Meeting*, 1989., pp. 579-587.

[9] K.T. Hung and R.D. Lorenz, "A Rotor Flux Error-Based, Adaptive Tuning Approach for Feedforward Field Oriented Induction Machine Drives", *1990 IEEE Industry Applications Soc. Annual Meeting*, October 1990.

[10] K.T. Hung, "A Slip Gain Error Model-Based Correction Scheme of Near-Deadbeat Response for Indirect Field Orientation", *Master Thesis*, University of Wisconsin-Madison, 1990.

[11] J.C. Moreira, "A Study of Saturation Harmonics with Applications in Induction Motor Drives", *Ph.D. Thesis*, University of Wisconsin-Madison, 1990.

[12] J.C. Moreira and T.A. Lipo, "A New Method for Rotor Time Constant Tuning in Indirect Field Oriented Control", *1990 IEEE Power Electronics Specialists Conference*, June 10-15, 1990, San Antonio, Texas.